Low-level cadmium doses do not jeopardize the insulin secretion pathway of β-cell models until the onset of cell death

Jean-Marc Moulis, Inès Nahoui-Zarouri, Marine Lénon, Cécile Cottet-Rousselle

Version of Record: https://www.sciencedirect.com/science/article/pii/S0946672X21001243
Manuscript_4305f5553eeb1f740f29a54acddfd822

Low-level cadmium doses do not jeopardize the insulin secretion pathway of β-cell models until the onset of cell death.

Jean-Marc Moulis[a,b], Inès Nahoui-Zarouri[b], Marine Lénon[b,1], Cécile Cottet-Rousselle[b]

[a] Univ. Grenoble Alpes, CEA, IRIG, 38000 Grenoble, France

[b] Univ. Grenoble Alpes, INSERM U1055, Laboratory of Fundamental and Applied Bioenergetics (LBFA), and Environmental and System Biology (BEeSy), 38000 Grenoble, France

Short title: Lack of functional impairment of β-cell models with low cadmium doses

Corresponding author. *Jean-Marc Moulis, Laboratory of Fundamental and Applied Bioenergetics (LBFA), INSERM U1055-University Grenoble Alpes, CS 40700; F-38058 Grenoble Cedex 9, FRANCE. Tel. +33 (0)476758598*
jmmoulis@protonmail.com

[1] ***Present address.*** Marine Lénon, Pasteur Institut, Stress Adaptation and Metabolism in enterobacteria Unit (SAMe), 28 rue du Docteur Roux, F-75015 PARIS, FRANCE. marine.lenon@pasteur.fr; Tel. +33 (0)186 46 79 08

Abstract

Background: Cadmium is an inescapable environmental pollutant that permeates the food chain and has been debatably associated with diabetes in humans.

Purpose and Procedures: To probe the specific impact of low-level cadmium exposure on insulin production, largely sub-cytotoxic (50 – 500 nM) concentrations of cadmium chloride challenged the INS-1 and MIN6 rodent models of pancreatic β-cells for the longest possible time, up to 4 days, before sub-culturing.

Main Findings: The concentration of detectable oxidants, the pattern of the actin cytoskeleton, the translocation of β-catenin, the activity of protein phosphatases, calcium traffic, and the phosphorylation status of several key signaling nodes, such as AMP kinase and mitogen activated kinases including nuclear translocation of Extracellular signal-Regulated Kinase, were all insensitive to the applied very low cadmium doses. Accordingly, low-level cadmium exposure did not alter the insulin secretion ability, the functional hallmark of β-cells, before the onset of cell death.
Conclusions: These data define an operational toxicological threshold for these cellular models of β-cells that should be useful to address insulin secretion and the diabetogenic effects of chronic low-level cadmium exposure in animal models and in humans.

Keywords

β-cells, diabetes, low-level exposure, threshold, glucose homeostasis, cadmium

Abbreviations

DCF: 2′,7′-Dichlorofluorescin diacetate; DHE: Dihydroethidine = 2,7-Diamino-10-ethyl-9-phenyl-9,10-dihydrophenanthridine, 3,8-Diamino-5,6-dihydro-5-ethyl-6-phenylphenanthridine; Fluo-4: 2-[2-[2-[2-[bis(carboxymethyl)amino]-5-(2,7-difluoro-3-hydroxy-6-oxoxanthen-9-yl)phenoxy]ethoxy]-N-(carboxymethyl)-4-methylanilino]acetic acid; Fura-2: 2-[6-[bis(carboxymethyl)amino]-5-[2-[2-[bis(carboxymethyl)amino]-5-methylphenoxy]ethoxy]-1-benzofuran-2-yl]-1,3-oxazole-5-carboxylic acid; Fura Red: acetyloxymethyl 2-[N-[2-(acetyloxymethoxy)-2-oxoethyl]-2-[2-[[6-[bis[2-(acetyloxymethoxy)-2-oxoethyl]amino]-2-[(E)-(5-oxo-2-sulfanylideneimidazolidin-4-ylidene)methyl]-1-benzofuran-5-yl]oxy]ethoxy]-4-methylanilino]acetate; GSIS: Glucose-Stimulated Insulin Secretion; H89: N-[2-[[3-(4-Bromophenyl)-2-propenyl]amino]ethyl]-5-isoquinolinesulfonamide; HEPES: 4-(2-Hydroxyethyl)piperazine-1-ethanesulfonic acid ; JC-1 ((5,5’,6,6’-tetrachloro-1,1’,3,3-tetraethylbenzimidazolylcarbocyanine iodide); LD 50: median lethal dose; Tfam: mitochondrial transcription factor A; TMRM ((tetramethylrhodamine methyl ester perchlorate)

1. Introduction

Despite intense interest, the actual impact of cadmium contamination on human and animal health remains controversial, except in a few instances of relatively high exposure, as in occupational activities of workers in specific areas (*e.g.*, mining, welding, battery manufacturing). In addition to cadmium inhalation by smokers, dietary ingestion derives from manure and phosphate fertilizers (1) that sustain intensive farming, and from eating seafood, particularly mollusks and shellfish, that accumulate cadmium even from lightly contaminated areas. A decade ago, the Tolerable Weekly Intake (TWI) was re-adjusted in Europe to 2.5 µg cadmium/ (kg body mass) (2), a value half the previous Provisional Tolerable Weekly Intake of 7 µg cadmium/ (kg body mass).

The variety of the potential molecular targets of cadmium (3) and their likely differential sensitivities to the actual modes of exposure (4) do not help settling disputes over the impact of environmental cadmium on health. Impaired glucose homeostasis leads to pre-diabetes and diabetes (5-7) and pancreatic β-cells are the specialized cells sensing increased glucose and responding to it by insulin secretion. The diabetogenic property of cadmium was clearly identified in animal models long ago (8), as was the correlation between cadmium exposure and increased blood glucose (9). However, the number of suspected underlying molecular and cellular mechanisms remains too large to properly assess their actual relevance at chronic low-doses (10-12). A large survey nailed down a dose-response relationship between urinary cadmium levels for people without evidence of pre-existing renal defects, and an increased risk of prediabetes (impaired fasting glucose) and type II diabetes (13). Subsequently, the complexity of such correlations has failed, up to now, to provide a clear-cut answer to the issue (5-7).

Most data usually report cadmium effects under experimental conditions that overlap with the onset of cell death. Hence, they do not provide insight on the most sensitive molecular targets of the toxic metal that may be disconnected from death pathways. Herein, the focus has rather been put on largely sub-lethal cadmium concentrations, and it appears that β-cell models do not show obvious signs of functional impairment up to a dose inducing cellular death.

2. Materials and Methods

The detailed sources of reagents are listed in Supplementary Table 1.

2.1. Cell cultures and exposure to cadmium.

INS-1 cells are derived from a rat insulinoma and they are used as models of pancreatic β cells, including because they keep the ability to produce and secrete insulin (14). Cells were obtained from the Department of Genetic Medicine and Development, University of Geneva Medical Center. They were kept in a humidified chamber with a 5% CO_2-95% air mixture at 37°C and maintained in RPMI 1640 medium containing 2 g/L of glucose (PAN Biotech) and supplemented with 10% fetal bovine serum (Biowest, Nuaillé - France), antibiotics (1% of 10000 U/mL penicillin and 10 mg/mL streptomycin), 70 µM 2-mercaptoethanol, 1 mM sodium pyruvate, and 2 mM glutamine. MIN6 cells are from a mouse insulinoma (15), and they were grown in Dulbecco's Modified Eagle's Medium-high glucose 4.5 g/L, supplemented with 10% fetal bovine serum, 2 mM L-glutamine, 100 UI/mL de penicillin, 100 µg/mL streptomycin and 50 µM 2-mercaptoethanol. Stock solutions of cadmium chloride ($CdCl_2$) were prepared in Phosphate Buffered Saline. Cells were cultured either in complete medium or in complete medium containing $CdCl_2$ at the desired concentration and incubated at 37°C with 5% CO_2 for 96 hours with one medium

change after 48 hours. The $CdCl_2$ treatment was started when cells were at ca. 30% confluence. Since the chosen cadmium concentrations did not impinge on viability and we did not want to involve any passage of the cells before analysis, harvest had to occur after 4 days at most, *i.e.*, when cells approached confluence.

The methods described in the following can be applied to both INS-1 and MIN6 cell lines, so that 'cells' will refer to both.

2.2. Estimates of reactive oxygen species concentration in cells.

Cells were seeded, left to adhere for 3 days, and treated with the indicated $CdCl_2$ concentrations for 48 h. The cadmium-containing medium was replaced, and the cells were kept for an additional 48 h. Viability was checked by trypan blue staining, cells were harvested, and 5 x 10^5 cells were labeled with 10 µM Dihydroethidium (Hydroethidine DHE, Molecular Probes - Invitrogen) or dihydrodichlorofluorescein diacetate acetyl ester (H_2DCF-DA, Molecular Probes - Invitrogen) before fluorescence recording on a LSR Fortessa^{TM} cell analyzer (Becton Dickinson) as previously described (16).

2.3. Viability measurements.

The proportion of viable cells was determined with the (3-[4, 5-dimethylthiazol-2-yl]-2, 5-diphenyl tetrazolium) bromide (MTT) method as previously described (17). LD 50 values were calculated by iteration with a four parameters logistic equation. The associated standard error, t and P values are approximations computed at the final iteration of the regression as implemented in the SigmaPlot v.11 (Systat Software, Inc.) package. The H89 concentration applied over the 4-day duration of the experiments was chosen in preliminary studies, and it is not cytotoxic in the absence of cadmium.

2.4. Separation of sub-cellular fractions.

Rinsed cell pellets were suspended in 3 pellet volumes of hypotonic buffer (Supplementary Table 1) and left at 4°C for 10 min. The suspensions were centrifuged at 1300 *g* for 15 min, 4°C, and the supernatants were kept as cytosolic lysates. The pellets were dispersed in 0.5 volume of low salt buffer then 0.5 volume of high salt buffer was added. The suspensions were agitated (20 rpm) at room temperature for 30 min, and centrifuged at 17000 *g* for 45 min to separate the soluble fraction (nuclei) from the membranes. The protein concentration of each fraction was measured before loading equal amounts on polyacrylamide gels.

2.5. Western Blots.

Cell lysates (30 µg of proteins per lane) were subjected to electrophoresis on polyacrylamide gels of concentrations adjusted to the size of the proteins of interest, and transferred to 0.2 µm polyvinylidene difluoride membranes using the TransBlot Turbo Blotting System (Bio-Rad) with a transfer program adjusted to the properties of the samples. Membranes were blocked with 5% bovine serum albumin in Tris Buffered Saline - 0.1% Tween-20 for 1 hour, washed, and incubated with primary antibodies solutions in the blocking buffer overnight at 4°C. Washed membranes were then incubated with goat anti-rabbit IgG- horseradish peroxidase conjugated secondary antibody for 1 hour, and complexes were visualized with the ECL™ Western Blotting Detection system (GE Healthcare Life Sciences). The generated luminescence was recorded with an ImageQuant LAS 4000 CCD camera (GE Healthcare Life Sciences).

For successive probing with different antibodies, membranes were stripped by a previously described method (18). The primary antibodies, listed in Supplementary Table 1, were routinely used at the 1:1000 dilution.

2.6. Immunofluorescence Measurements.

These experiments were carried out as previously reported (16) using the same primary antibodies as for Western blot analysis described above but diluted 1:200. The secondary antibody was 200-fold diluted goat anti rabbit secondary antibody Hylite Fluor® 488 (Anaspec– Fremont, CA, USA), and micrographs were recorded with a Leica TCS SP8 inverted laser scanning confocal microscope (Leica Microsystems, Wetzlar, Germany) equipped with a 40x oil immersion objective (Leica HC PL APO 40x/1.30 Oil CS2). F-actin labeling was with DyLight 488 conjugated phalloidin (Thermo Scientific 21833). Image analysis was carried out with the Image J (imagej.nih.gov) and Volocity (Improvision, Perkin-Elmer, Courtaboeuf, France) computer programs. Briefly, tophat filtering in Image J was applied to the phalloidin images. This filter extracts intense peaks over background, depending on size and shape criteria. This filtering technique allows the removal of noise and the precise extraction of filamentous objects as cytoskeleton filaments. Regions of interest were chosen in each series, and the Volocity software provided the skeletal length of the objects in the filtered images.

2.7. Measurement of insulin secretion.

Cells were seeded at *ca*. 3 x 10^6 in 6 mL of medium and treated with cadmium as described above in 25 cm^2 flasks at 37°C and 5% of CO_2 for 96 h. Cells were pre-incubated in low glucose (0.5 g/L = 2.8 mM) medium overnight. They were washed with phosphate buffered saline, and the medium was replaced by 2.5 mL of the

Krebs Ringer Buffer (Supplementary Table 1), containing 1 mg/mL bovine serum albumin with either 0.5 g/L (2.8 mM) or 4.5 g/L (25 mM) glucose, and the cells were kept at 37°C for one hour. The supernatants were recovered for insulin measurements, the cells were lysed and their protein content was determined.

The insulin concentrations in the cell supernatants were measured by the homogenous time resolved fluorescence (HTRF) Insulin assay (CisBio Bioassays, Codolet, France). The reaction was carried out with 2.5 µL of 10- and 15-fold diluted collected supernatants added to 37.5 µL of the Eu^{3+} cryptate (fluorescence donor) and XL665 (acceptor) antibodies as instructed by the provider. Each sample was distributed in two wells of a 384-well white plate and incubated overnight at room temperature. The emitted fluorescence at 620 and 665 nm with 330 (10) nm excitation was measured with a BMG-Labtech Clariostar multimode reader with 60 µs delay and 400 µs integration time. This assay conveniently detects insulin in the 10-150 ng/mL range.

2.8. Measurement of the cAMP concentration

The cAMP assay similarly used the HTRF technology with the anti-cAMP- Eu^{3+} cryptate antibody and the cAMP-d2 fluorescence acceptor (CisBio Bioassays). The raw data were normalized to the protein concentration of each sample in lysates of *ca*. 2.5 x 10^5 cells.

2.9. Mitochondrial transmembrane potential and cellular reducing potential.

Two probes with different diffusion coefficients were used to estimate the mitochondrial transmembrane potential (ΔΨ) with the BMG-Labtech Clariostar multimode reader. Mitochondrial aggregated JC-1 ((5,5',6,6'-tetrachloro-1,1',3,3-tetraethylbenzimidazolylcarbocyanine iodide) was measured at exc/em = 535 (15) /

595 (20) nm, whereas its monomeric form was at 485 (15) /530 (20) nm. TMRM ((tetramethylrhodamine methyl ester perchlorate) probe was detected at 544 (15) /590 (20) nm. Cells were seeded at 2 x 10^5 cells/well in a 96-well plate, and treated with cadmium as described above in quadruplicate. At the end of the cadmium treatment cells were washed and loaded in the dark with 1.5 µM JC-1 or 15 nM TMRM for 90 and 15 min, respectively. The fluorescence measurements were normalized to the amount of nucleic acids in each well which was measured with the SYBR® Gold nuclear stain (ThermoFisher Scientific).

2.10. Relative estimate of messenger RNA.

Total RNA was purified using the High Pure RNA isolation kit (Roche). Complementary DNA (cDNA) was synthesized from 1 µg of total RNA with M-MuLV reverse transcriptase (Euromedex, Souffelweyersheim, France) and the oligo $(dT)_{12-18}$ primer. The diluted cDNA was amplified by real time qPCR (Agilent Aria Mx) with the HOT Pol EVAGreen qPCR Mix Plus (Euromedex) and primers validated for rat β-actin, Cyclophilin A, and hypoxanthine guanine phosphoribosyl transferase, as normalizing genes, and rat insulin (Supplementary Table 2).

2.11. Measurement of Protein Phosphatase Activity.

Cells (1 x 10^6) in 25 cm^2 flasks were exposed to cadmium as described above. At the end of the treatment cells were harvested and lysed in 10 mM HEPES, pH 7.5, 3 mM $MgSO_4$, 15 mM KCl, 2% glycerol, 0.2% NP-40 with 250 µM tris carboxyethyl phosphine and a mix of protease inhibitors at 4°C for 15 minutes. Aliquots of the supernatants were transferred to a 96 well plate. The protein phosphatase activity of the lysate was measured in 150 µL containing 750 µM of para nitro phenyl phosphate (pNPP) for one hour. The reaction was stopped by adding 45 µl of 10 M NaOH, and

the absorbance was measured at 405 nm in the BMG-Labtech Clariostar multimode reader.

2.12. Measurement of calcium flux.

Cells were inoculated at 3 x 10^4 /well in 96-well µClear plates (Greiner Bio One International GmbH) and exposed to cadmium as described above. After washing, cells were loaded with Fura-2-AM (ThermoFisher Scientific) 8 µM in Tyrode buffer (Supplementary Table 1) with 1 mg/mL bovine serum albumin, and the chosen concentrations of glucose and calcium for 1 hour at 37°C. Substrates, inhibitors, and other additives were added with the injectors of the BMG-Labtech Clariostar multimode reader, and the Fura-2 fluorescence was recorded from below the plate by excitation at 340 nm (Ca-Fura-2 complex) and 380 nm (Ca-free Fura-2) with fluorescence emission detected using a 510–520 nm band pass filter. Alternatively, Fluo-4-AM (ThermoFisher Scientific) and Fura Red-AM (ThermoFisher Scientific) were used and loaded at 2 and 4 µM, respectively, as for Fura-2, but for 45 min at room temperature. The corresponding fluorescence was recorded at exc/em 483 (14) / 530 (30) and 488 (20) / 640 (40) nm with the same instrument. In each experiment verapamil or calcymycin were added to some wells before glucose to verify that stimulation no longer changed the slope of the fluorescence changes.

2.13. Statistical analysis.

The results were analyzed for each applied cadmium concentration with reference to non-treated cells. The data were subjected to One Way Analysis of Variance tests with the SigmaPlot (Systat Software, Inc.) statistical module, and the significance level was set at 0.05.

3. Results

Most experiments reported below were obtained with samples of the two INS-1 and MIN6 cell lines, but most figures were drawn with the results obtained with INS-1. One exception is the viability of MIN6 cells in the presence of Cd^{2+} that was not reported before under the present conditions in contrast to INS-1 cells. The other is the localization of β–catenin that was monitored for MIN6 cells, which was not changed by the applied low-level cadmium concentrations (*vide infra*) and was not investigated further as any possible variation in other cells could not be generalized. In all cases, no differences in the measured parameters relative to non-treated cells, taken as reference, were found between the two cell lines when exposed to largely sub-lethal doses of cadmium.

3.1 Impact of cadmium on the viability of β-cells models and determination of the targeted dose-range

In the case of rodent pancreatic INS-1 β-cells, it was established that sub-µM concentrations of cadmium in the growth medium did not induce significant cell death in between medium changes since the LD 50 was of the order of 5 µM under these conditions (16). MIN6 cells also display LD 50 in the low µM range, at 1.8 µM in the presently implemented conditions (*vide infra*). Therefore, the following experiments have been carried out with sub-µM Cd^{2+} concentrations added to the growth medium for 4 days. These experiments follow the longest protocol that can be applied to the cell lines between passages, and they constitute a follow-up of a recent report in which cadmium was shown to accumulate inside INS-1 cells long before viability decreased (16). If the study were carried out for longer times with several passages with renewal of the cadmium charge, cadmium would accumulate inside cells over time. It would be thus expected that the cadmium concentration needed to trigger cell

death would decrease because of the longer exposure. Under such conditions, potential early molecular changes induced by low-level cadmium would be missed.

3.2 Do β-cells models experience increased levels of reactive oxygen species at low cadmium doses?

The association between cadmium exposure and oxidative stress has been largely documented, in insulin secreting cells in particular (19,20). Fluorescent probes are often used to detect the presence of cellular oxidants. Here, dichlorofluorescein (DCF) and dihydroethidium (DHE) were used to estimate whether sub-lethal cadmium doses increased the intra-cellular concentration of oxidants. In agreement with previous measurements using DHE in INS-1 cells (16), the applied range of cadmium doses did not generate species that significantly react with DCF or DHE (Fig. 1).

Mitochondria are often a source of oxidants, leaking from the respiratory chain for instance, thus the absence of obvious DCF or DHE oxidation (Fig. 1) is also congruent with the constant energetic charge and O_2 respiration devoted to ATP production at sub-lethal doses of cadmium applied to INS-1 cells (16). The function of INS-1 mitochondria is thus preserved before viability is jeopardized (16). Accordingly, neither the Tfam transcription factor regulating mitochondrial DNA transcription, mitogenesis, and mitochondrial function (Fig. 2A), nor the estimated mitochondrial membrane potential with either the JC-1 or TMRM markers (shown for TMRM in Fig. 2B) changed as a function of the applied cadmium sub-lethal dose.

3.3 Are chronic low-level cadmium doses affecting insulin secretion by β-cells models?

Pancreatic β-cells are specialized in granular insulin excretion, and one may wonder whether low-level cadmium exposure might dedifferentiate the studied model systems. To examine this point, the amount of Pdx1 (Pancreatic Duodenal Homeobox-1), the transcriptional activator of insulin, was evaluated by immuno-blotting and shown to be constant as a function of the cadmium dose in the chosen sub-lethal range (Fig. 3A). Accordingly, the transcription of the insulin gene did not change with the applied cadmium concentration (Fig. 3B). This implies that the sub-lethal long-term cadmium treatment does not perturb the quantity of the insulin transcript in β-cells.

The potential impact of low-level cadmium exposure on insulin secretion was further investigated by comparing the amounts of insulin secreted by cells in a given time lapse after glucose stimulation. Preliminary experiments were carried out to ensure that no lysis occurred during the secretion assay, as this would spoil the measurements. The data are reported here as the stimulation index which is the ratio of the insulin quantities produced under high glucose conditions (25 mM) and the non-stimulated excretion (2.8 mM glucose). Fig. 4 indicates that, within the precision range that can be obtained in such measurements, this important functional parameter of β-cells is insensitive to the presence of intra-cellular cadmium at levels insufficient to trigger cell death (One-way ANOVA $p = 0.285$). The stimulation index remains largely above 1, which demonstrates that these cells can be similarly stimulated by glucose all over the applied cadmium concentration range.

3.4 Which signaling pathways might be sensitive to low cadmium doses in β-cells models?

In view of the reported impact of cadmium treatments on the cytoskeleton in various cell types (21), we wondered whether rearrangement of the F-actin filaments

occurred in the presence of low doses of cadmium. Indeed, the dynamics of the cytoskeleton, which is under the dependence of the PAK1 signaling pathway, plays a critical role in insulin exocytosis (22,23). Fig. 5 shows that the actin network, including the peripheral F-actin filaments holding insulin granules, is not significantly disordered by the accumulation of cadmium in the applied conditions until the onset of cell death at 2 µM cadmium (Fig. 5).

Despite the lack of functional consequences of low cadmium doses on the β-cells models studied here, these cells may accommodate the cadmium insult by triggering some signaling pathway allowing them to maintain their insulin secretion properties. Indeed, the mechanism of insulin secretion involves a succession of glucose- and other secretagogues-triggered reactions leading to exocytosis of insulin granules under the dependence of various regulatory systems. Impairment of one of these molecular pathways may be counterbalanced by other mechanisms without changing the secreting properties of the cells.

1) Cadmium has been shown to disrupt adherens junctions of epithelial cells by interfering with the E-Cadherin-β-catenin complex due to the interaction of cadmium divalent ions with E-cadherin (24). At relatively acute cadmium levels, nuclear translocation of β-catenin yielded transcriptional upregulation of some of its targets (25). Here, long-term exposure of β-cell models to less than 0.5 µM $CdCl_2$ failed to evidence any displacement of β-catenin (Fig. 6). This result indicates integrity of the cell-cell interactions and lack of differences in β-catenin signaling with the cadmium treatment until the onset of cell death, *i.e.,* largely below 2 µM.

2) Cadmium has been reported to potently inhibit protein tyrosine phosphatases (26), but the importance of this effect in insulin producing cells is unknown. Indeed, considering the role of phosphorylation reactions in insulin production and secretion

by β-cells, it seems legitimate to look for interference by cadmium. The protein phosphatase activity of cells exposed to low concentrations of cadmium for 4 days was not found to vary significantly (ANOVA test *p* between groups = 0.207) as a function of the cadmium concentration, up to that leading to the onset of cell death (Fig. 7).

3) The potential sensitivity of β-cells to low concentrations of cadmium applied for 4 days was further probed in the absence and in the presence of H-89, a protein kinase inhibitor that efficiently targets protein kinase A (PKA). Under such conditions, the LD 50 in the absence of inhibitor was 1.8 (Standard Error 0.1) µM for MIN6 cells. The viability curves were not changed by the presence of the H89 inhibitor, hence excluding the involvement of PKA and other H89-sensitive signaling pathways in the cellular response to low level cadmium concentrations (Fig. 8A). Accordingly, measurements of the PKA-activating second messenger cAMP did not reveal any change as a function of the applied sub-lethal cadmium concentrations in INS-1 cells within the precision range attainable for these measurements (Fig. 8B).

4) Cadmium can interfere with calcium signaling including because both cations have similar ionic radii (3). Insulin exocytosis relies on massive intra-cytoplasmic calcium increase due to plasma membrane depolarization after closing of potassium channels. The calcium flux, either with the Fura-2 ratiometric probe or with the combination of Fluo-4 and Fura Red, was monitored with glucose stimulation in cadmium-exposed cells (Fig. 9). Increasing exposure to cadmium below LD 50 was not sufficient to perturb the increase of intra-cellular calcium concentration triggered by glucose stimulation (One-way ANOVA $p = 0.887$). This result is congruent with the lack of changes of the insulin secretion rates observed above (Fig. 4).

The effects of cadmium on signaling cascades are numerous, and many of them are associated with a change of the cellular redox balance (27). At cadmium concentrations below 0.5 µM applied for 4 days, cell death (Fig. 8A) and increased oxidant concentrations (Fig. 1) are not observed. If a cadmium insult were associated with the implemented exposure conditions, some signaling pathways may detect it. Besides translocation of cadherin presented above (Fig. 6), the phosphorylation status of AMPK, JNK/SAPK, p38, AKT, and mTOR did not vary. Similarly, phosphorylation of ERK1/2 was not significantly changed by long-term (for 4 days) exposure to cadmium at low (≤0.5 µM) concentrations (Fig. 10). However, it has to be noticed that the standard deviation of these measurements, which involve between 6 and 14 different cultures for each INS-1 and MIN6 cell lines, increases above 250 nM Cd^{2+} as compared to lower cadmium concentrations. This may impinge on the high sensitivity of ERK signaling to a variety of signals, but no dose dependence with the cadmium concentration could be unambiguously evidenced in these experiments. Furthermore, invariance with low-level cadmium exposure holds both in the conventional culture medium and for glucose-stimulated cells. This was also verified by fluorescence microscopy with labeled antibodies monitoring nuclear translocation of the ERK isoforms and their phosphorylated derivatives that trafficked independently of the applied cadmium concentration (Fig. 11).

4. Discussion

It has been known for a long time that the mechanisms of action of cadmium, and other toxic chemicals, on pancreatic β-cells depend on the pollutant concentration and the duration of exposure as recently recalled (28). Interference between cadmium and calcium uptake for instance was studied long ago, and low calcium was shown to favor cadmium uptake (29), but the impact of cadmium on insulin secretion

could not be explained, or not only, by impairment of calcium traffic (30). Cadmium accumulation in islets of exposed mice was less than that measured in exocrine pancreas (29), but cadmium uptake does occur in β-cell models, *e.g.,* (16,19,20). From the above quoted data and many other studies, pancreatic β-cells and their cellular models cannot be confidently considered as sensitive targets of cadmium toxicity comparatively to other cell types. Considering this knowledge gap, we probed early molecular evidence of disturbance in pathways related to glucose homeostasis by application of largely sub-cytotoxic cadmium conditions to two representative β-cell models. The implemented experiments examined the cell morphology, various markers of stress, such as the presence of oxidants and the activation of stress-responsive signaling pathways, and insulin secretion, the specialized main function of β-cells. Our data show that variations of all these parameters were associated with cell death, without any obvious precursory indication of molecular changes at very low cadmium doses.

This conclusion contrasts with some other sub-toxic chemical treatments of pancreatic β-cells, such as with tributyltin for which insulin secretion and signaling pathways were perturbed (31). For cadmium, short-term (24 h) exposure to 5 µM (28,32) or longer-term (up to 48 h) exposure to >0.1 µM (20) of cell models inhibited glucose stimulated insulin secretion (GSIS). Accordingly, decreased GSIS correlated with increased cell death in the RIN-m5F cell model (19).

Remarkably, the effects of cadmium on insulin secretion were found to become significant at concentrations above those increasing fluorescent probe-detected oxidant species or decreasing viability in one study (19), whereas such features were not reported in other investigations (20,28). This emphasizes the importance of the choice of the parameters used to monitor the toxicity of a given compound, all the

more so as the functional assay characterizing β-cells (insulin secretion) may not always recapitulate the structural or other effects of the pollutant (16,19). This observation suggests that β-cells may protect their most important function despite cadmium accumulation within some limited range, hence the possibility of showing some sort of functional threshold (33). Yet, the mechanism of safe cadmium storage in β-cells is not known. The present experimental design with insulinoma cell models is characterized by the length of the cadmium exposure without dissociation and harvest of these adherent cells, a procedure that implies stress. Cadmium exposure for 4 days largely, by a factor of at least 2, exceeds the exposure time used in most previous studies. Our measurements failed to demonstrate obvious changes of a diversity of molecular pathways that were potential targets of low-level cadmium doses. It can then be inferred that the widely used β-cell models are examples of cells that adapt to low cadmium concentrations without apparent damage and display features that differ depending on the length of exposure (34). Indeed, the present work and a previous one (16) show that very few features are modified before the onset of cell death.

One may argue that the relatively large standard deviations associated with some experiments reported herein hide the presence of changes in the measured parameters (Type II error). However, no specific trends of the mean values appear on any of the probed properties: if a drift occurs with the cadmium dose that may have been missed, it must be modest and with relatively little functional consequences particularly for insulin secretion (Fig.4). With this limitation in mind, we conclude that the presently implemented conditions rather points toward the medium-term insensitivity of β-cells models to sub-lethal cadmium doses.

The presently reported data have to be compared with observations made with animal models, notwithstanding the necessarily different doses applied in both cases. It was recently observed (35,36) that very low-level cadmium intoxication of rats led to sex specific differences and developmental dependence of glucose homeostasis. Glucose homeostasis of young rats exposed to low-level cadmium through their lightly intoxicated mothers relied on several parameters (36). The glucose tolerance tests of pups at weaning, were modeled (37), and the results suggested that the β-cells-response in the slow phase of insulin secretion to increased glucose at weaning was impaired by previous low-level cadmium exposure *in utero* and during lactation. However, it is difficult to closely compare the data obtained upon exposing naïve organisms to low-level cadmium doses. Pups were exposed via their mothers for a long time and during development including early stages of pancreas maturation. and the β-cell models overlook these aspects. Furthermore, the β-cell lines were obtained from cancerous tissue of adult animals and grown on glucose, whereas lipids are the major type of substrate for pancreatic islets of weaning pups.

Instead of evidencing high sensitivity to cadmium, our data suggest that insulin secretion by isolated β-cells is not a function readily affected by cadmium in fully developed animals (35). Thus, studies like the present one, instead of pointing to an additional pathway contributing to impaired insulin secretion in partly damaged cells, set an experimental framework suitable to probe glucose homeostasis under mild cadmium stress, in the presence of additional stressors/toxicants for instance (38). However, the conclusions reached with cellular models like the ones used herein should not be stretched too far in explaining observations made with experimental animals or human populations. But at least they provide a well calibrated set-up that

is useful to evaluate the respective contributions to multi-factorial detrimental conditions, such as disturbed glucose homeostasis and diabetes.

Acknowledgements

The authors thank the contribution of several undergraduate students who contributed to the work as partial fulfillment of their degrees. This research was supported by a grant from Agence Nationale de la Recherche France (ANR-13-CESA-008-Cadmidia). The funding agency had no involvement in the collection, analysis and interpretation of data; in the writing of the report; and in the decision to submit the article for publication.

Declarations of interest: none

Figures Captions

Fig. 1

Cadmium-triggered fluorescence of oxidative species probes in INS-1 cells. Cells were grown in the presence of cadmium and loaded with either DHE or DCF as described in Materials and Methods. The cell suspensions were analyzed and the fluorescence of ethidium (left) and dichlorofluorescein (right) were recorded. The dashed lines mark the maximum of the histogram without cadmium and they are meant to guide the eye through the panels.

Fig. 2

A. Representative Western Blot of Tfam. Western blots of 30 µg of INS-1 lysates exposed to varying cadmium concentrations probed successively with anti-Tfam and anti-β-actin antibodies. Arrows on the right indicate the position of size markers.
B. Mitochondrial membrane potential. The histogram represents the results of experiments carried out with INS-1 cells labeled with TMRM. The cells were treated as described (Materials and Methods), and the values of the measured fluorescence were normalized with the fluorescence of SYBR Gold-labeled nucleic acids, hence corrected for the number of cells present in the corresponding well. One way analysis of variance failed to suggest statistically significant differences ($p = 0.345$).

Fig. 3

A. Representative Western Blots of Pdx1. Protein lysates from the two INS-1 and MIN6 cell lines exposed to the indicated concentrations of cadmium were successively probed with anti-Pdx1 (top) and anti-actin (bottom) antibodies. The mass of the two visible standards in the lane labeled ‘markers’ are from the Precision Plus Protein WesternC standards (Bio-Rad) at 37 and 50 kDa.

B. Relative quantities (RQ) of the insulin mRNA. The qPCR data from INS-1 cells exposed to the indicated concentrations of cadmium are reported relative to the 3 housekeeping genes used to normalize the data. One way ANOVA analysis failed to evidence any significant difference across the cadmium concentration range.

Fig. 4

Insulin secretion index. The insulin concentration in the cellular supernatants of INS-1 cells treated with the indicated cadmium concentrations was measured by HTRF (Materials and Methods) after incubation for one hour in low (0.5 g/L) and high (4.5 g/L) glucose conditions. The values were normalized to the protein amount present in each sample, hence proportional to the number of cells. The data shows the means of the ratios of normalized insulin concentrations excreted by stimulated and non-stimulated cells for each applied cadmium concentration. One way analysis of variance did not return a statistically significant difference among groups ($p = 0.285$)

Fig. 5

A. Representative micrographs of the cytoskeleton of INS-1 cells. The images were recorded after 4 days of Cd^{2+} exposure (Materials and Methods), and they are displayed with green for DyLight 488 conjugated phalloidin and red for nuclei labeled with propidium iodide. The Cd^{2+} concentrations (in nM) are indicated on the left of the panels. Scale bar: 10 µm.

B. Plot of the average filament length (in nm) as a function of the cadmium treatment. The values were calculated for 3 areas of cells for each condition (Materials and Methods). Only the cells submitted to 2 µM Cd^{2+} display a significantly different value (<0.05) from the non Cd exposed cells.

Fig. 6

β-catenin localization after exposure to low-level concentrations of cadmium. Top: the cell fractions from cadmium-exposed MIN6 cells were analyzed by immunoblot with the anti β-catenin antibody after polyacrylamide 4-15% gel electrophoresis. The leftward lane of each blot contains molecular markers with the 100 and 80 kDa bands. Equal loading was ensured by measurements of protein concentrations, and checked for the cytosolic fraction with β–actin (not shown). Bottom: micrographs of β-catenin-labeled cells (red) and nuclear staining with Hoechst 33258 (blue) after the indicated treatments with Cd^{2+}. The picture at 2 µM is shown to illustrate the damage the cells endure at the onset of cell death. Scale bar: 10 µm.

Fig. 7

Protein phosphatase activity of cadmium-exposed β-cell models. The activity of protein phosphatases on the pNPP substrate was measured with lysates of INS-1 cells exposed to the indicated cadmium concentrations for 4 days (Materials and Methods).

Fig. 8

A. Sensitivity of the MIN6 β-cell model to exposure to cadmium. Viability was measured with MTT for MIN6 cells supplemented with 10 nM H89 and grown with increasing cadmium concentrations for 4 days (open symbols). The same data in the absence of H89 is shown for comparison (black symbols). The left-most symbol (0 Cd - 100%) is common to both conditions. Standard deviations for 6 measurements are plotted as error bars, and 4-parameter logistic fits (lines, black for MIN6 cells, red with H89) did not evidence significant differences in the calculated LD 50 values.
B. cAMP concentration in cadmium exposed INS-1 cells. The cAMP concentration of cells was determined as described (Materials and Methods) and plotted with the standard deviations of 6 measurements.

Fig. 9

Stimulation of calcium influx by glucose. INS-1 cells previously exposed to low-level cadmium were loaded with Fluo-4 and Fura Red, stimulated with 19.4 mM glucose, and the kinetics of calcium traffic were recorded (Materials and Methods). The plotted values are the means of the rates of calcium uptake in relative fluorescence units with SD. One way analysis of variance did not evidence any statistically significant difference ($p = 0.887$).

Fig. 10.

Top: Phosphorylation status of the Extracellular signal-Regulated Kinase (p44/p42 MAPK). Top: INS-1 cells were exposed to cadmium for 4 days as described and their lysates were analyzed by Western Blot. The data are reported as the ratio of the phosphorylated/total forms of the protein, and the basal value for cells not exposed to cadmium is arbitrarily set to 1. The data are the results of at least 6 biological replicates for each cadmium concentration and they did not provide a statistically significant difference among groups (P = 0,589). Bottom: representative Western Blots used to draw the above histogram. The sizes of the molecular markers (kDa) are indicated on the left.

Fig. 11.

Nuclear translocation of p44/p42 MAPK (ERK) in INS-1 cells. Micrographs were recorded after labeling cells with Dylight 488 fluorescent secondary antibodies binding to primary ones directed against either ERK (A) or P-ERK (C). Nuclei were stained with propidium iodide (PI). Scale bar: 10 µm. The proportion of ERK (B) and P-ERK (D) fluorescence found in the nuclear volume is plotted with SD in the histograms as a function of the cadmium treatment. Neither plot corresponded to a significant difference among groups, ($P > 0.05$).

References

1. Imseng M, Wiggenhauser M, Keller A, Muller M, Rehkamper M, Murphy K, Kreissig K, Frossard E, Wilcke W, Bigalke M. Fate of Cd in Agricultural Soils: A Stable Isotope Approach to Anthropogenic Impact, Soil Formation, and Soil-Plant Cycling. Environ Sci Technol 2018;52(4):1919-1928.
2. EFSA. Cadmium in food. Scientific Opinion of the Panel on Contaminants in the Food Chain. EFSA Journal 2009;980:1-139.
3. Moulis JM, Bourguignon J, Catty P. Cadmium. In: Maret W, Wedd A, editors. Binding, Transport and Storage of Metal Ions in Biological Cells, RSC Metallobiology. Cambridge, UK: Royal Chemical Society; 2014. p 695-746.
4. Callegaro G, Forcella M, Melchioretto P, Frattini A, Gribaldo L, Fusi P, Fabbri M, Urani C. Toxicogenomics applied to in vitro Cell Transformation Assay reveals mechanisms of early response to cadmium. Toxicology in vitro : an international journal published in association with BIBRA 2018;48:232-243.
5. Guo FF, Hu ZY, Li BY, Qin LQ, Fu C, Yu H, Zhang ZL. Evaluation of the association between urinary cadmium levels below threshold limits and the risk of diabetes mellitus: a dose-response meta-analysis. Environ Sci Pollut Res Int 2019;26(19):19272-19281.
6. Kuo CC, Moon K, Thayer KA, Navas-Acien A. Environmental chemicals and type 2 diabetes: an updated systematic review of the epidemiologic evidence. Current diabetes reports 2013;13(6):831-849.
7. Tinkov AA, Filippini T, Ajsuvakova OP, Aaseth J, Gluhcheva YG, Ivanova JM, Bjorklund G, Skalnaya MG, Gatiatulina ER, Popova EV, Nemereshina ON, Vinceti M, Skalny AV. The role of cadmium in obesity and diabetes. The Science of the total environment 2017;601-602:741-755.
8. Merali Z, Singhal RL. Diabetogenic effects of chronic oral cadmium adminstration to neonatal rats. Br J Pharmacol 1980;69(1):151-157.
9. Bell RR, Early JL, Nonavinakere VK, Mallory Z. Effect of cadmium on blood glucose level in the rat. Toxicol Lett 1990;54(2-3):199-205.
10. Jacquet A, Ounnas F, Lenon M, Arnaud J, Demeilliers C, Moulis JM. Chronic Exposure to Low-Level Cadmium in Diabetes: Role of Oxidative Stress and Comparison with Polychlorinated Biphenyls. Curr Drug Targets 2016;17(12):1385-1413.
11. Moulis JM, Thevenod F. New perspectives in cadmium toxicity: an introduction. Biometals 2010;23(5):763-768.
12. Thevenod F, Lee WK. Toxicology of cadmium and its damage to mammalian organs. Metal ions in life sciences 2013;11:415-490.
13. Schwartz GG, Il'yasova D, Ivanova A. Urinary cadmium, impaired fasting glucose, and diabetes in the NHANES III. Diabetes Care 2003;26(2):468-470.
14. Asfari M, Janjic D, Meda P, Li G, Halban PA, Wollheim CB. Establishment of 2-mercaptoethanol-dependent differentiated insulin-secreting cell lines. Endocrinology 1992;130(1):167-178.
15. Miyazaki J-I, Araki K, Yamato E, Ikegami H, Asano T, Shibasaki Y, Oka Y, Yamamura K-I. Establishment of a Pancreatic β Cell Line That Retains Glucose-Inducible Insulin Secretion: Special Reference to Expression of Glucose Transporter Isoforms. Endocrinology 1990;127(1):126-132.
16. Jacquet A, Cottet-Rousselle C, Arnaud J, Julien Saint Amand K, Ben Messaoud R, Lenon M, Demeilliers C, Moulis JM. Mitochondrial Morphology and Function of the Pancreatic beta-Cells INS-1 Model upon Chronic Exposure to Sub-Lethal Cadmium Doses. Toxics 2018;6(2).

17. Rousselet E, Richaud P, Douki T, Garcia-Chantegrel J, Favier A, Bouron A, Moulis JM. A zinc-resistant human epithelial cell line is impaired in cadmium and manganese import. Toxicol Appl Pharmacol 2008;230(3):312-319.
18. Yeung YG, Stanley ER. A solution for stripping antibodies from polyvinylidene fluoride immunoblots for multiple reprobing. Analytical biochemistry 2009;389(1):89-91.
19. Chang KC, Hsu CC, Liu SH, Su CC, Yen CC, Lee MJ, Chen KL, Ho TJ, Hung DZ, Wu CC, Lu TH, Su YC, Chen YW, Huang CF. Cadmium Induces Apoptosis in Pancreatic beta-Cells through a Mitochondria-Dependent Pathway: The Role of Oxidative Stress-Mediated c-Jun N-Terminal Kinase Activation. PLoS One 2013;8(2):e54374.
20. El Muayed M, Raja MR, Zhang X, MacRenaris KW, Bhatt S, Chen X, Urbanek M, O'Halloran TV, Lowe WL, Jr. Accumulation of cadmium in insulin-producing beta cells. Islets 2012;4(6):405-416.
21. Choong G, Liu Y, Templeton DM. Interplay of calcium and cadmium in mediating cadmium toxicity. Chem Biol Interact 2014;211:54-65.
22. Kalwat MA, Thurmond DC. Signaling mechanisms of glucose-induced F-actin remodeling in pancreatic islet beta cells. Experimental & molecular medicine 2013;45:e37.
23. Zu Y, Gong Y, Wan L, Lv Y, Cui S, Jin X, Li C, Chen X. Pericentrin Is Related to Abnormal beta-Cell Insulin Secretion through F-Actin Regulation in Mice. PLoS One 2015;10(6):e0130458.
24. Prozialeck WC. Evidence that E-cadherin may be a target for cadmium toxicity in epithelial cells. Toxicol Appl Pharmacol 2000;164(3):231-249.
25. Edwards JR, Kolman K, Lamar PC, Chandar N, Fay MJ, Prozialeck WC. Effects of cadmium on the sub-cellular localization of beta-catenin and beta-catenin-regulated gene expression in NRK-52E cells. Biometals 2013;26(1):33-42.
26. Singh KB, Maret W. The interactions of metal cations and oxyanions with protein tyrosine phosphatase 1B. Biometals 2017;30(4):517-527.
27. Thévenod F, Lee WK. Cadmium and cellular signaling cascades: interactions between cell death and survival pathways. Archives of toxicology 2013;87(10):1743-1786.
28. Dover EN, Patel NY, Stýblo M. Impact of in vitro heavy metal exposure on pancreatic beta-cell function. Toxicol Lett 2018;299:137-144.
29. Nilsson T, Rorsman F, Berggren PO, Hellman B. Accumulation of cadmium in pancreatic beta cells is similar to that of calcium in being stimulated by both glucose and high potassium. Biochim Biophys Acta 1986;888(3):270-277.
30. Nilsson T, Berggren PO, Hellman B. Cadmium-induced insulin release does not involve changes in intracellular handling of calcium. Biochim Biophys Acta 1987;929(1):81-87.
31. Chen YW, Lan KC, Tsai JR, Weng TI, Yang CY, Liu SH. Tributyltin exposure at noncytotoxic doses dysregulates pancreatic beta-cell function in vitro and in vivo. Archives of toxicology 2017;91(9):3135-3144.
32. Beck R, Chandi M, Kanke M, Styblo M, Sethupathy P. Arsenic is more potent than cadmium or manganese in disrupting the INS-1 beta cell microRNA landscape. Archives of toxicology 2019;93(11):3099-3109.
33. Moulis JM, Bohat Z, Buha Djordjevic A. Threshold in the Toxicology of Metals: challenges and pitfalls of the concept. Current Opinion in Toxicology 2020;in press.
34. Moulis JM. Cadmium Exposure: Cellular and Molecular Adaptations. In: Uversky VN, Kretsinger RH, Permyakov EA, editors. Encyclopedia of Metalloproteins. New York, NY: Springer Science+Business Media; 2012.
35. Jacquet A, Arnaud J, Hininger-Favier I, Hazane-Puch F, Couturier K, Lenon M, Lamarche F, Ounnas F, Fontaine E, Moulis JM, Demeilliers C. Impact of chronic and low cadmium exposure of rats: sex specific disruption of glucose metabolism. Chemosphere 2018;207:764-773.
36. Jacquet A, Barbeau D, Arnaud J, Hijazi S, Hazane-Puch F, Lamarche F, Quiclet C, Couturier K, Fontaine E, Moulis JM, Demeilliers C. Impact of maternal low-level cadmium exposure on

glucose and lipid metabolism of the litter at different ages after weaning. Chemosphere 2019;219:109-121.
37. Rocca A, Fanchon E, Moulis JM. Theoretical analysis of oral glucose tolerance tests helps deciphering the impact of gestational cadmium exposure on the glucose homeostasis of offspring. Toxics 2020;in press.
38. Wang X, Mukherjee B, Park SK. Associations of cumulative exposure to heavy metal mixtures with obesity and its comorbidities among U.S. adults in NHANES 2003-2014. Environ Int 2018;121(Pt 1):683-694.

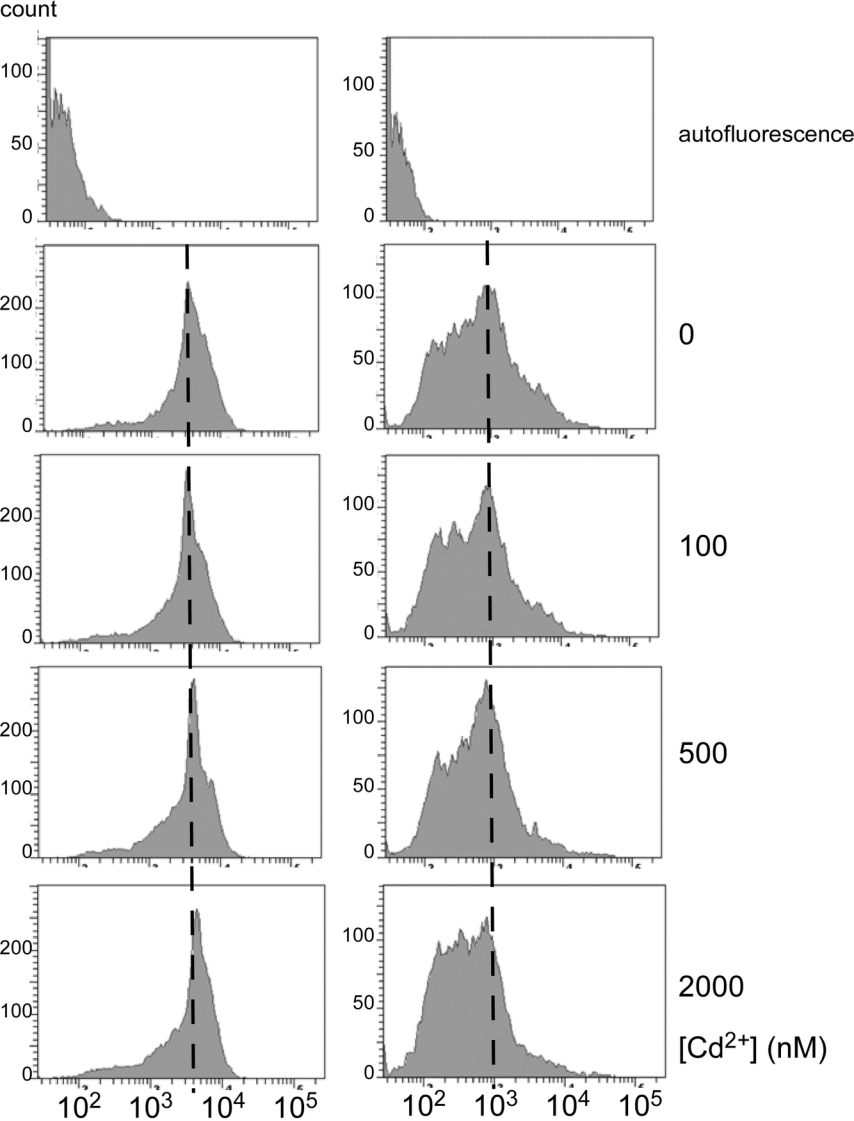
count
100
50
0
autofluorescence
200
100
0
0
100
500
2000
[Cd2+] (nM)
10^2
10^3
10^4
10^5
Ethidium fluorescence from DHE
DCF fluorescence

Figure 1

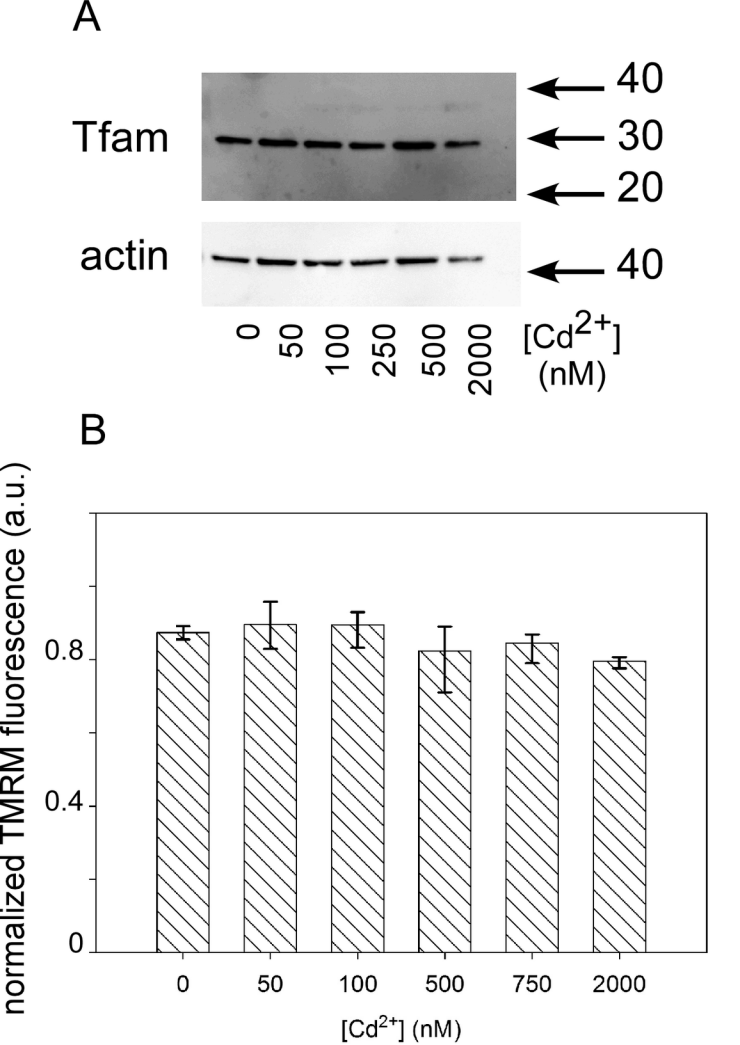
A
Tfam
actin
40
30
20
40
0
50
100
250
500
2000
[Cd2+]
(nM)
B
normalized TMRM fluorescence (a.u.)
0.8
0.4
0
0
50
100
500
750
2000
[Cd2+] (nM)

Figure 2

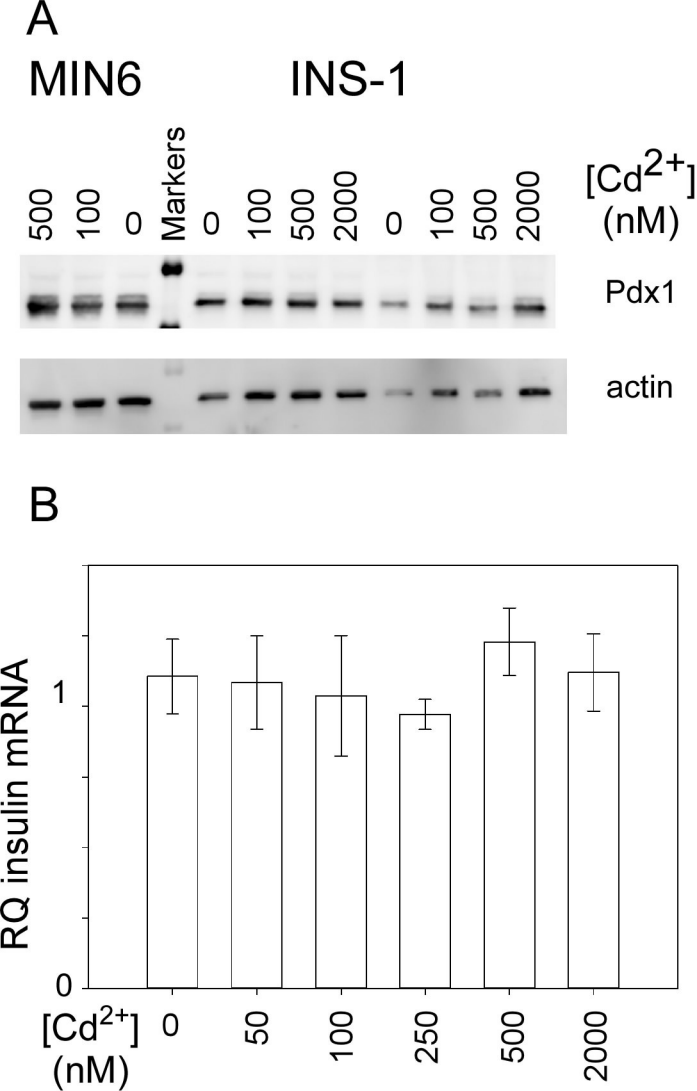
A
MIN6
INS-1
500
100
0
Markers
0
100
500
2000
0
100
500
2000
[Cd2+] (nM)
Pdx1
actin
B
RQ insulin mRNA
1
0
[Cd2+] (nM)
0
50
100
250
500
2000

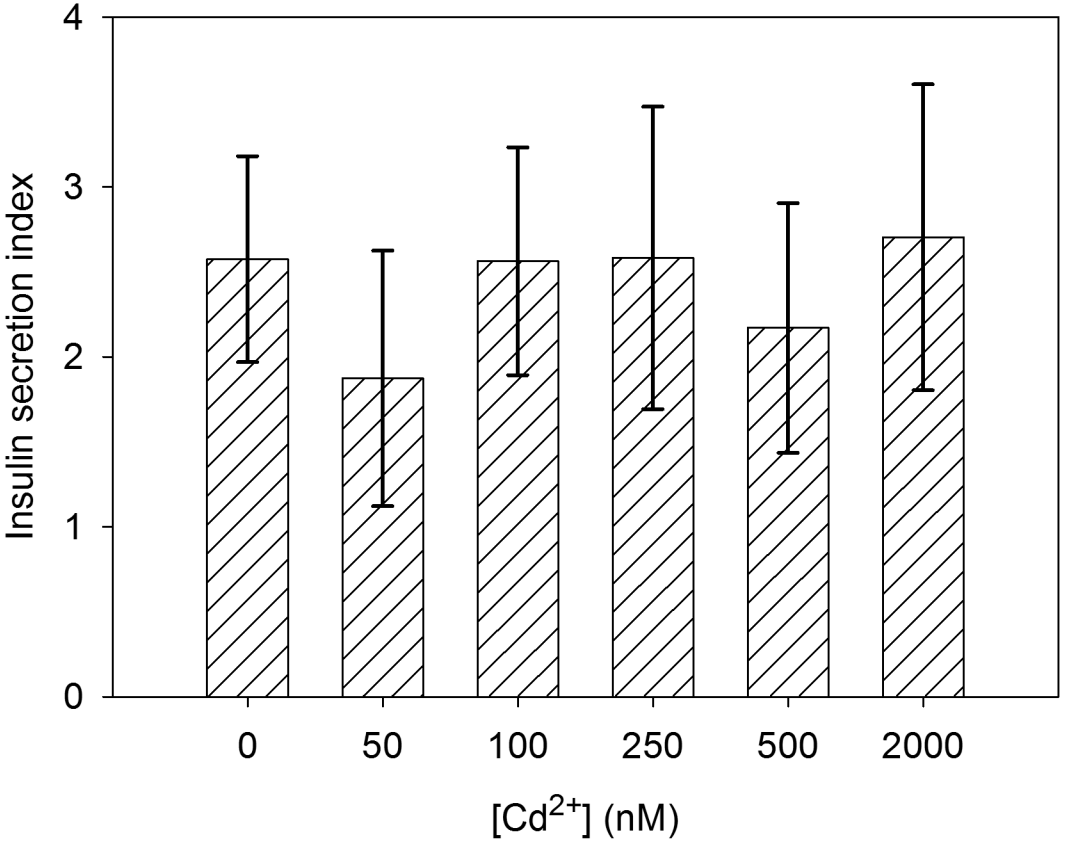

Figure 4

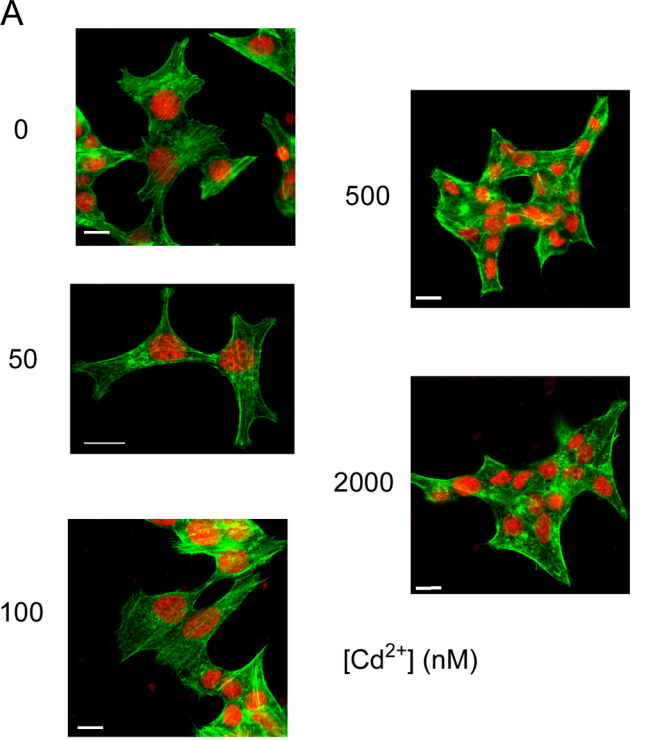
A
0
50
100
500
2000
[Cd2+] (nM)

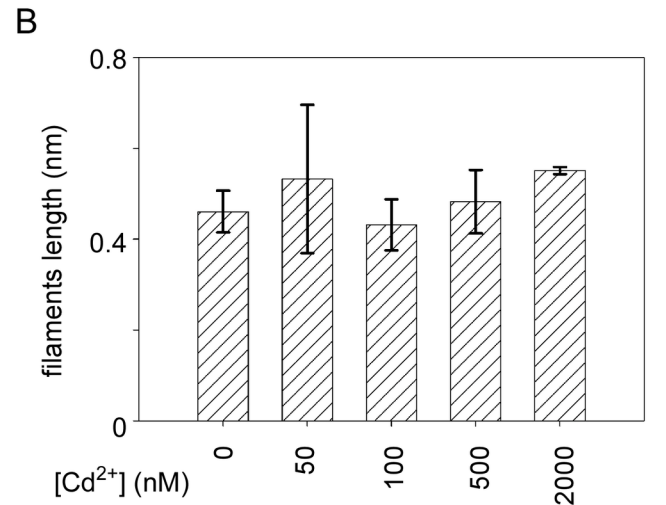
B
0.8
0.4
0
filaments length (nm)
0
50
100
500
2000
[Cd2+] (nM)

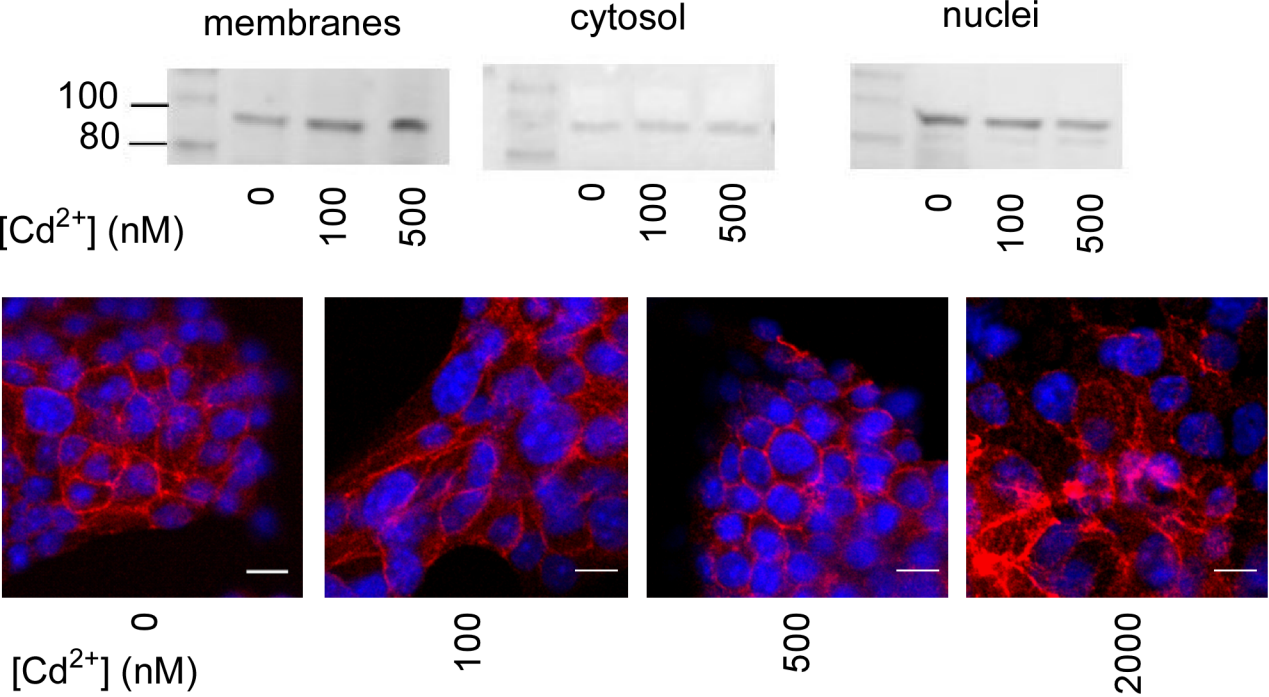
membranes
cytosol
nuclei
100
80
[Cd2+] (nM)
0
100
500
0
100
500
0
100
500
0
[Cd2+] (nM)
100
500
2000

Figure 6

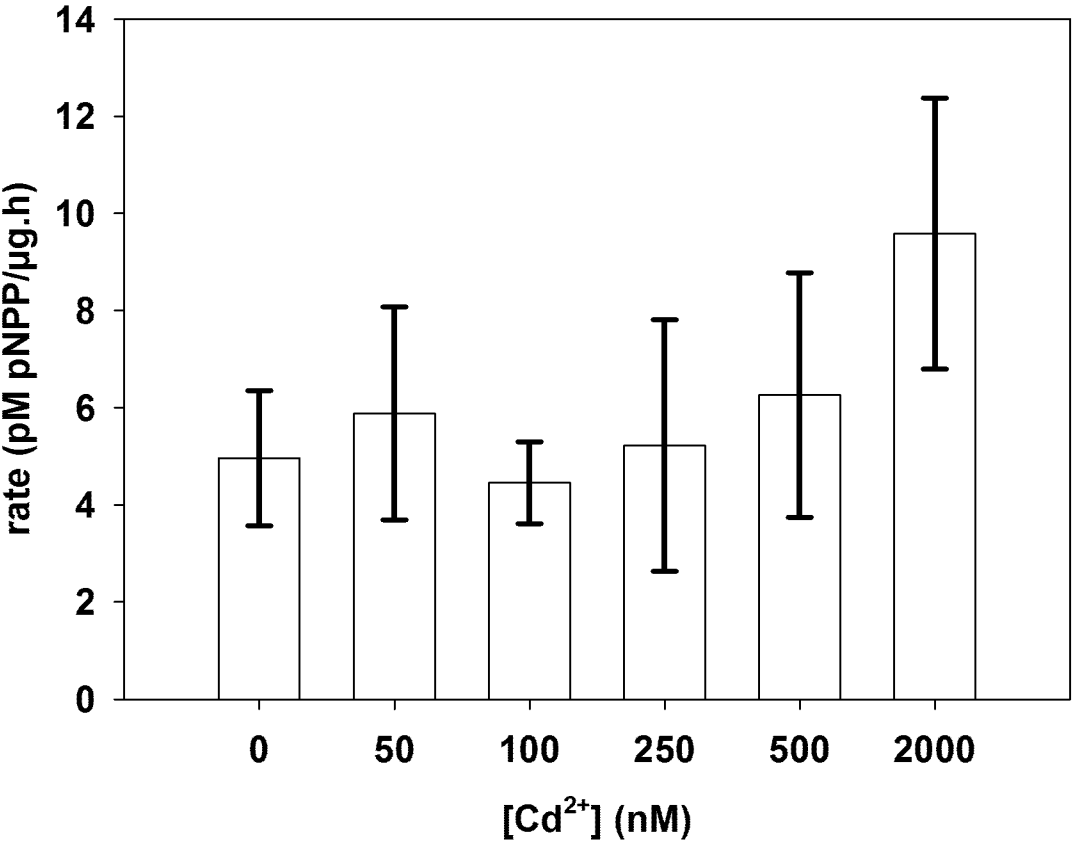

Figure 7

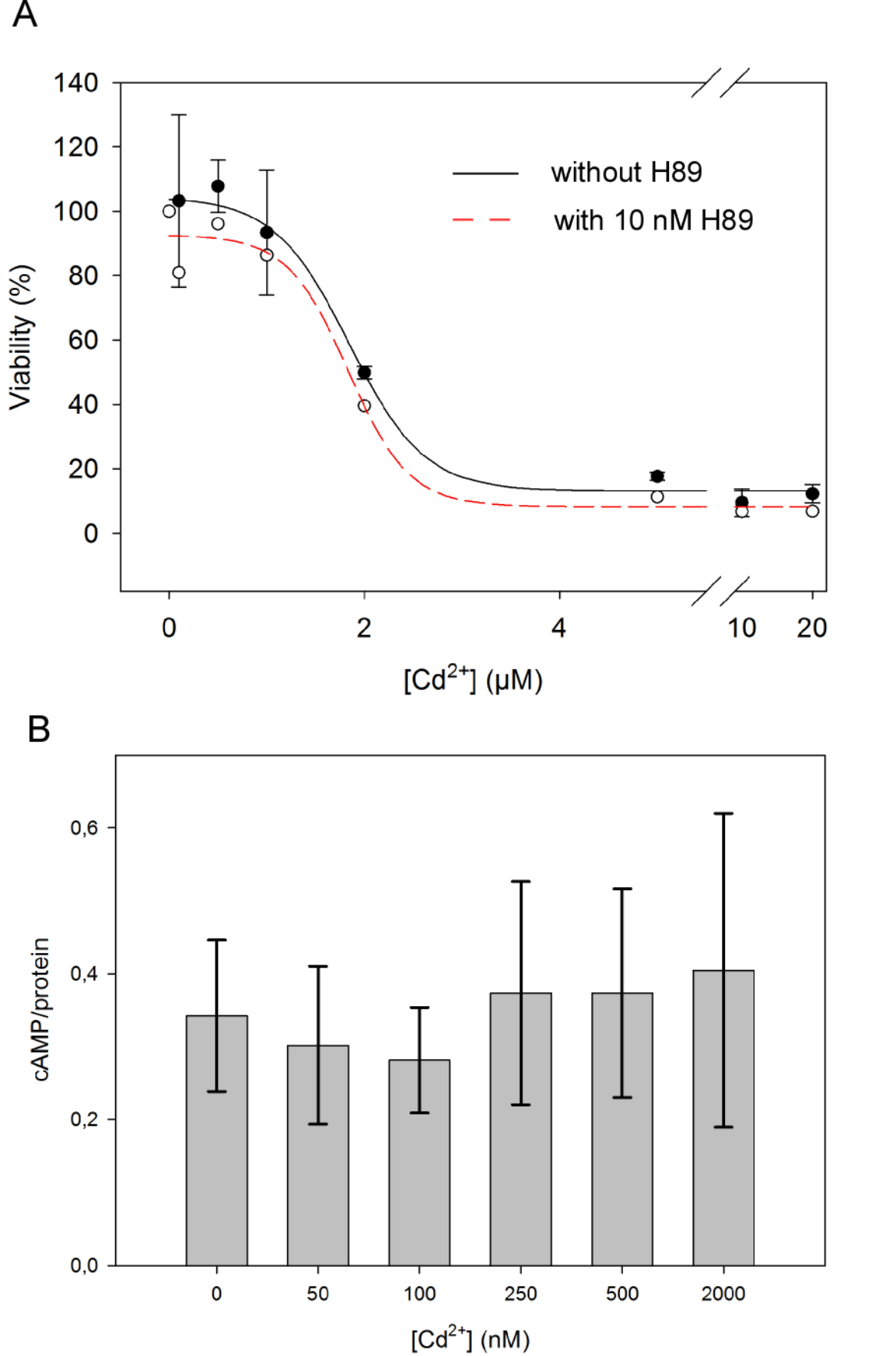
A
140
120
100
80
60
40
20
0
Viability (%)
without H89
with 10 nM H89
0
2
4
10
20
[Cd2+] (µM)
B
0,6
0,4
0,2
0,0
cAMP/protein
0
50
100
250
500
2000
[Cd2+] (nM)

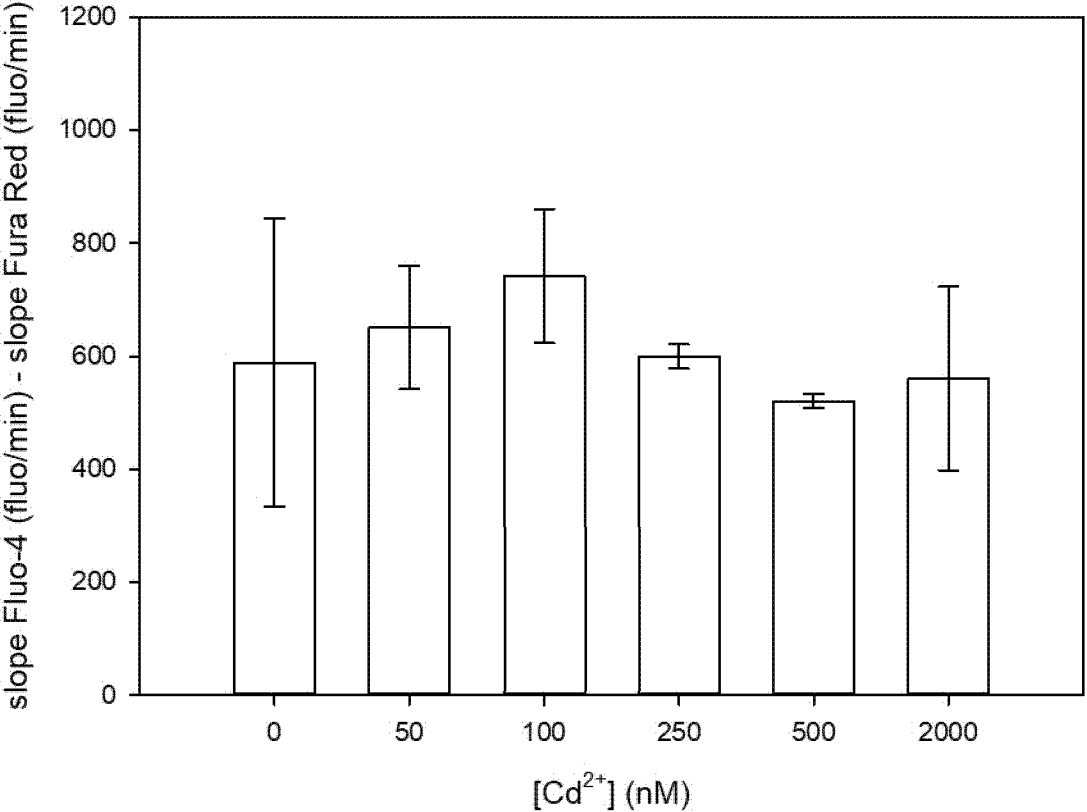
slope Fluo-4 (fluo/min) - slope Fura Red (fluo/min)
1200
1000
800
600
400
200
0
0
50
100
250
500
2000
[Cd2+] (nM)

Figure 9

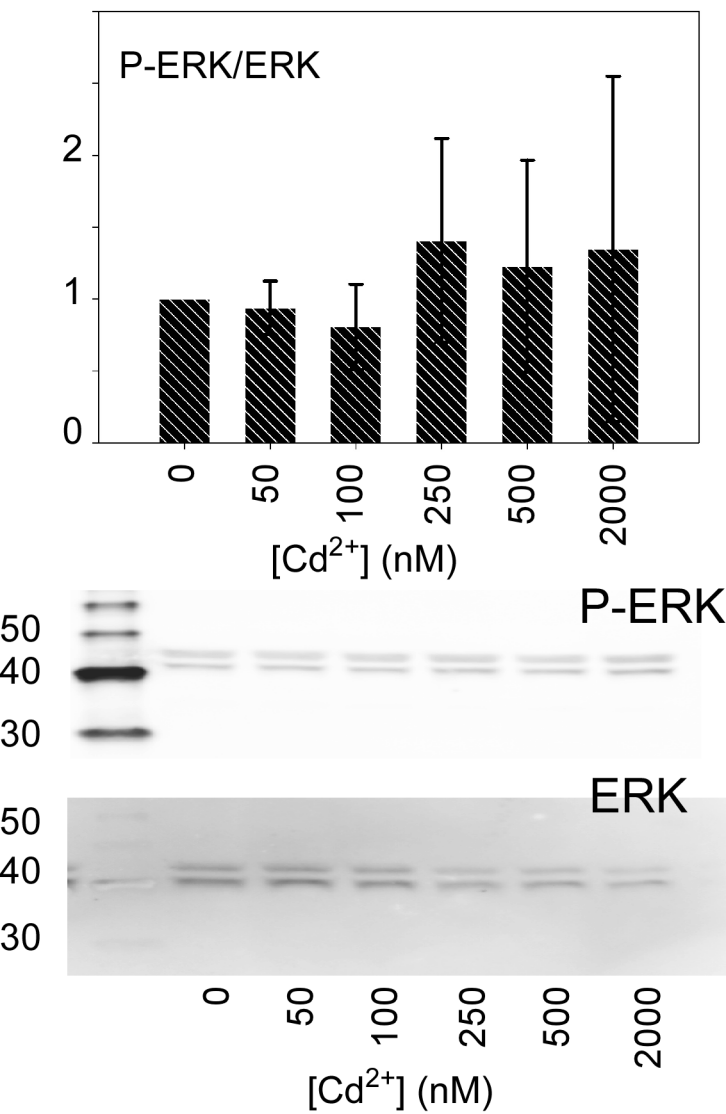
P-ERK/ERK
2
1
0
0
50
100
250
500
2000
[Cd2+] (nM)
P-ERK
50
40
30
ERK
50
40
30
0
50
100
250
500
2000
[Cd2+] (nM)

Figure 10

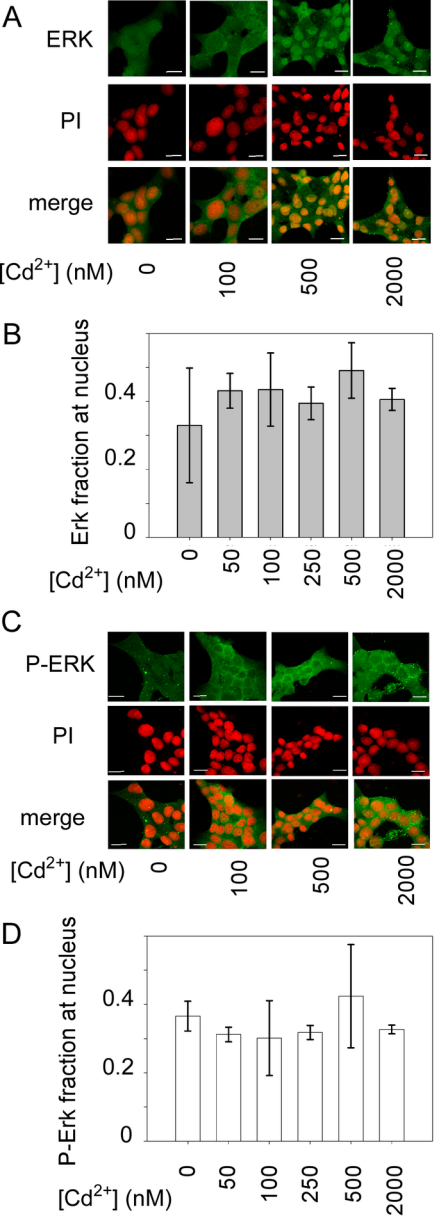
A
ERK
PI
merge
[Cd2+] (nM)
0
100
500
2000
B
Erk fraction at nucleus
0.4
0.2
0
0
50
100
250
500
2000
[Cd2+] (nM)
C
P-ERK
PI
merge
[Cd2+] (nM)
0
100
500
2000
D
P-Erk fraction at nucleus
0.4
0.2
0
0
50
100
250
500
2000
[Cd2+] (nM)

Figure 11

β-cell models

applied [Cd^{2+}] long exposure

[Cd^{2+}] intra

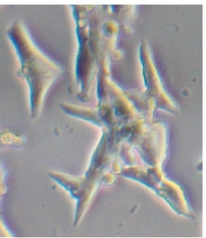

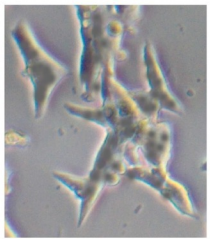

onset of cell death

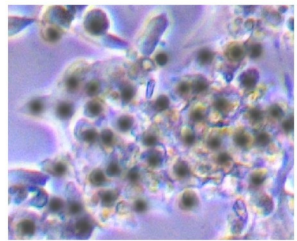

threshold

no changes

-morphology
-signaling pathways
-insulin secretion, ...

changes & damage